

Introduction

Non-uniform sampling (NUS) has been demonstrated to offer advantages over uniform sampling in the form of time savings, resolution enhancement, and, under some circumstances, sensitivity gains. We have developed a program containing a suite of regularization terms, including an ℓ_1 -norm regularization that utilizes a novel gradient descent method called NESTA [1], which is shown to converge in significantly fewer steps than related IST methods. This program, called NESTA-NMR [2], is able to reconstruct a 4D NMR spectrum in ~ 3 hours on a desktop computer.

A reconstruction enhancement method, called Gradient Assisted Virtual Echo (GrAVE), has been incorporated in NESTA-NMR and is demonstrated to produce accurate spin relaxation parameters, as determined from two-dimensional ^{15}N amide transverse relaxation time series (R_2), with sampling densities as low as 6% (32 complex points). These results are demonstrated on the *apo* form of the DNA binding domain of GCN4 from *S. cerevisiae*, which contains an intrinsically disordered region (IDR).

Theory

A Minimize $\|f\|_{\ell_1}$ subject to $Rx = b$,
using gradient Δf , where

$$\|f\|_{\ell_1} = \sum |f_k|$$

$$|f_k| = \sqrt{f_{k,r}^2 + f_{k,i}^2}$$

B Virtual Echo
Half-Dwell Delay = $\begin{bmatrix} R_1 & R_2 & \dots & R_N & R_N & \dots & R_2 & R_1 \\ I_1 & I_2 & \dots & I_N & -I_N & \dots & -I_2 & -I_1 \end{bmatrix}$

Virtual Echo
Zero-Dwell Delay = $\begin{bmatrix} R_1 & R_2 & \dots & R_N & 0 & R_N & \dots & R_3 & R_2 \\ 0 & I_2 & \dots & I_N & 0 & -I_N & \dots & -I_3 & -I_2 \end{bmatrix}$

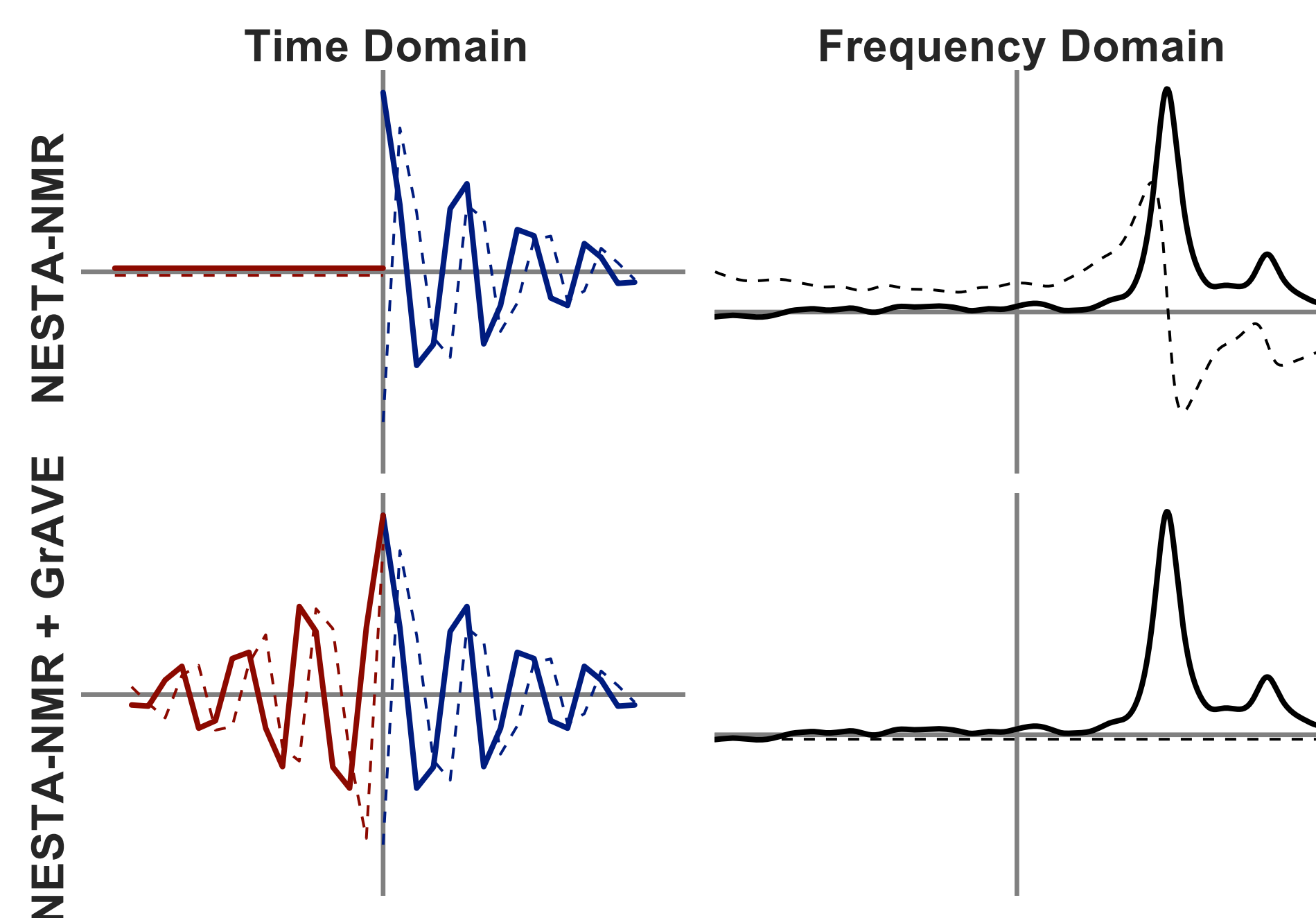


Figure 1. (A) The optimization performed by NESTA-NMR minimizes the ℓ_1 -norm of the spectrum, while ensuring the product of the sparse matrix of the sampled data (R) and the coefficients of the solution (x) are equal to a zero-filled matrix of the sampled data (b). (B) The virtual echo utilized in the gradient of NESTA-NMR is created by appending the time-reversed complex conjugate (red) onto the signal (blue). When the initial delay is zero, the signal is also shifted by one point. Virtual echo representations were adapted from Mayzel, *et. al* [3].

References

1. Becker S., Bobin J. & Candès E. (2011) *SIAM J. Imaging Sci.*, **4**, 1–39.
2. Sun S., Gill M., Yifei L., Huang M. & Byrd R.A. (2015) *J. Biomol. NMR*, **62**, 105–117.
3. Mayzel M., Kazimierczuk K. & Orekhov V.Y. (2014) *Chem. Commun.*, **50**, 8947–8950.
4. Ellenberger T.D., Brandl C.J., Struhl K. & Harrison S.C. (1992) *Cell*, **71**, 1223–1237.
5. Bracken C., Carr P.A., Cavanagh J. & Palmer A.G. (1999) *J. Mol. Biol.*, **285**, 2133–2146.

Acknowledgments

This work was supported by the Intramural Research Program of the National Institutes of Health, National Cancer Institute, Center for Cancer Research.

GCN4 Structure

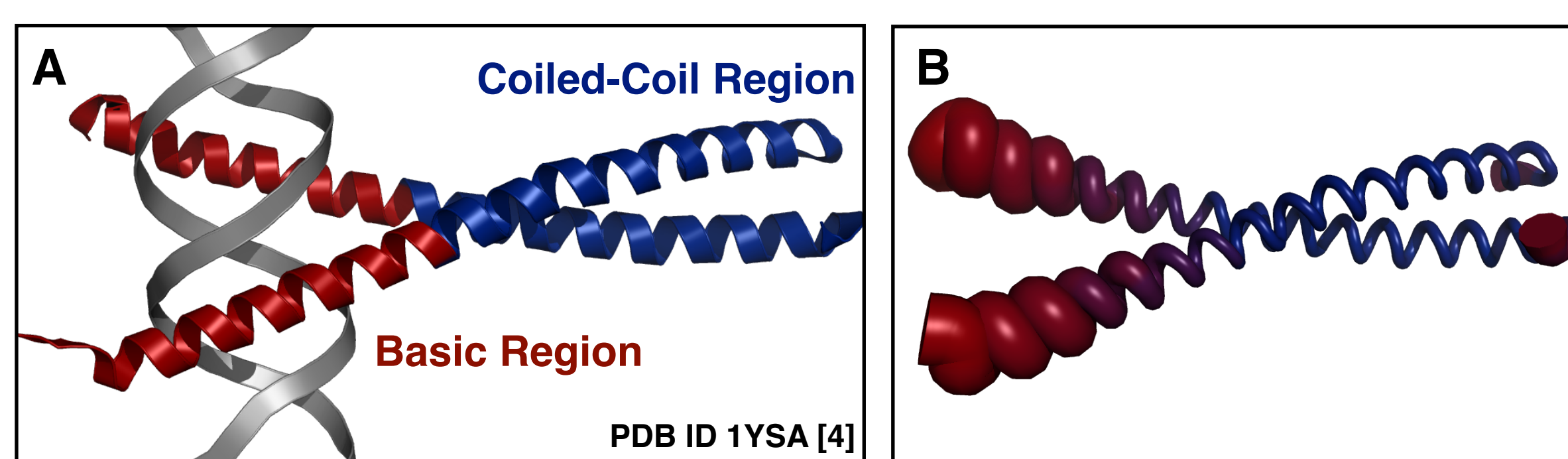


Figure 2. (A) The DNA binding domain of GCN4 contains an N-terminal basic region (red) and a C-terminal coiled-coil region (blue). (B) The basic region is disordered in the absence of DNA, as demonstrated by the order parameters (S^2) determined by Bracken, *et. al* [5], which are represented by the thickness of the backbone.

Reconstruction With GrAVE

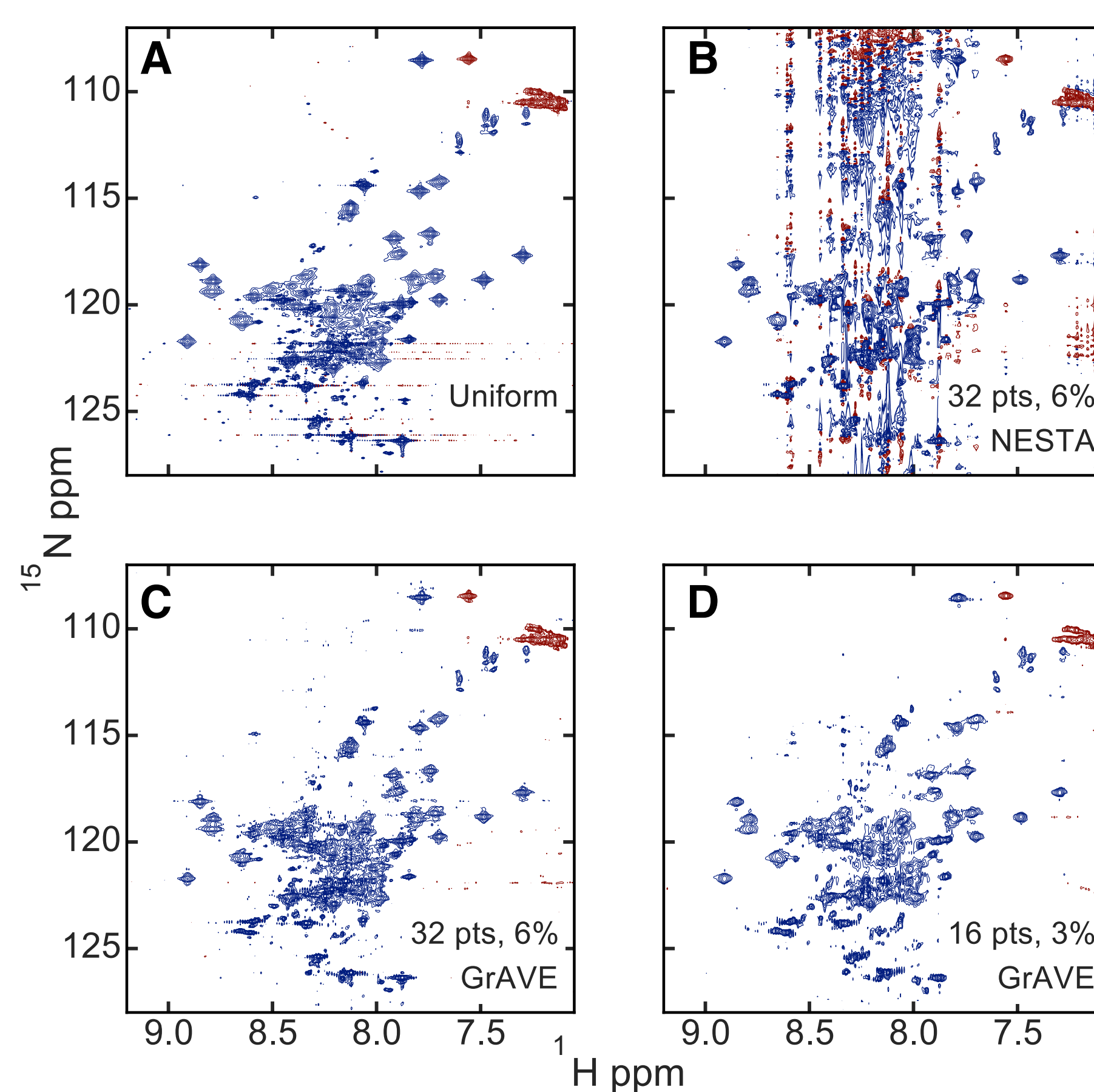


Figure 3. Comparison of uniformly sampled and NUS spectra of GCN4 from the first time point (4 ms) of a ^{15}N amide transverse spin relaxation experiment. (A) A uniformly sampled spectrum with 512 complex points. (B) A NUS spectrum with 32 complex points (6% sampling density) processed with NESTA-NMR. (C) The same sampling density as part B, but processed using NESTA-NMR with GrAVE. (D) A NUS spectrum with 16 complex points (3% sampling density) processed using NESTA-NMR with GrAVE.

Relaxation Rate Comparison (I)

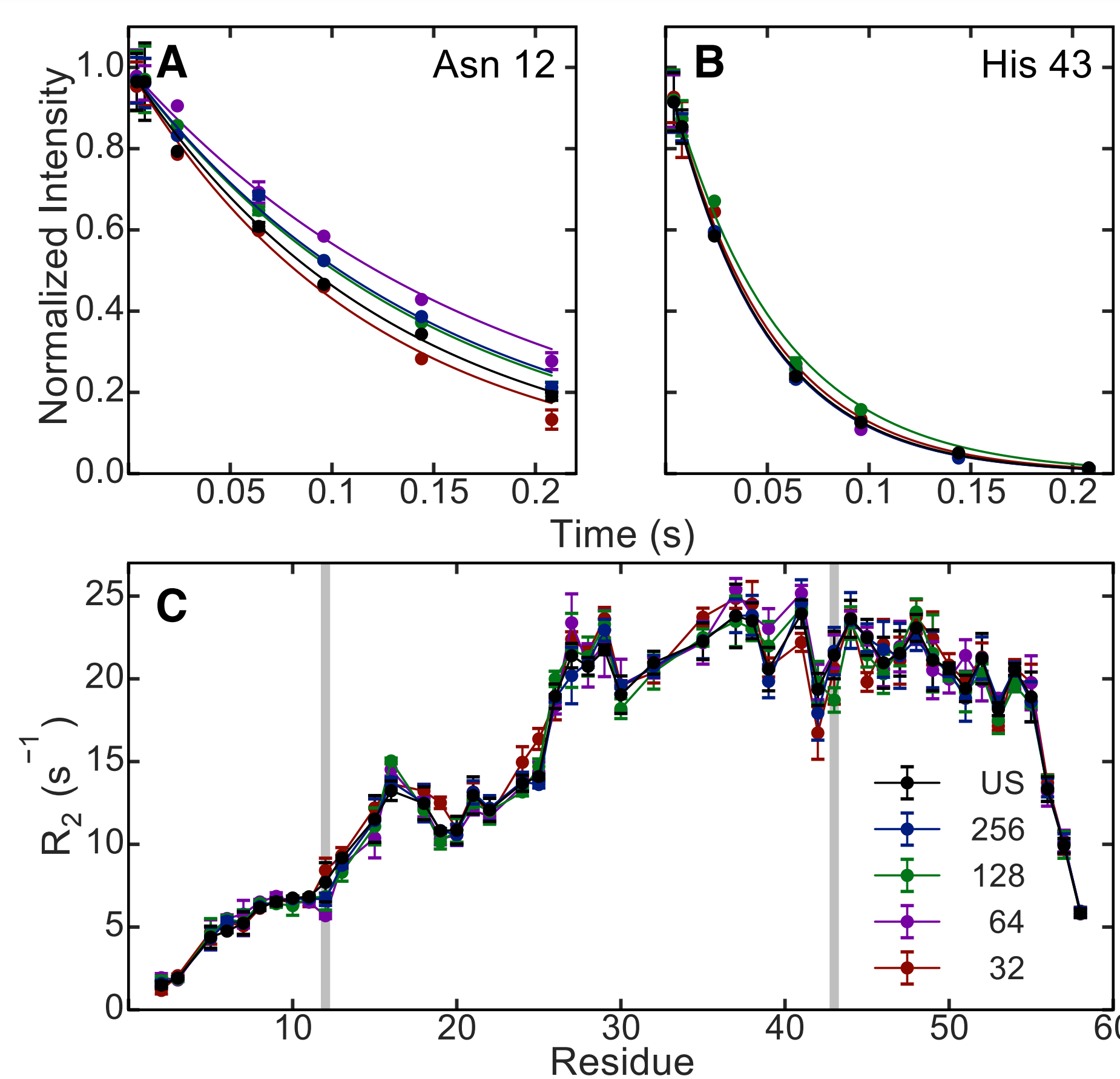


Figure 4. Comparison of transverse relaxation profiles and rate constants (R_2). ^{15}N amide spin relaxation decay profiles are shown for (A) Asn 12 in the disordered basic region and (B) His 43 in the coiled-coil region. (C) ^{15}N amide transverse relaxation rate constants for residues in GCN4. Colors represent uniformly sampled data (black) and NUS spectra containing 256 (blue), 128 (green), 64 (purple), and 32 (red) complex points that correspond to 50%, 25%, 13%, and 6% sampling density, respectively.

Relaxation Rate Comparison (II)

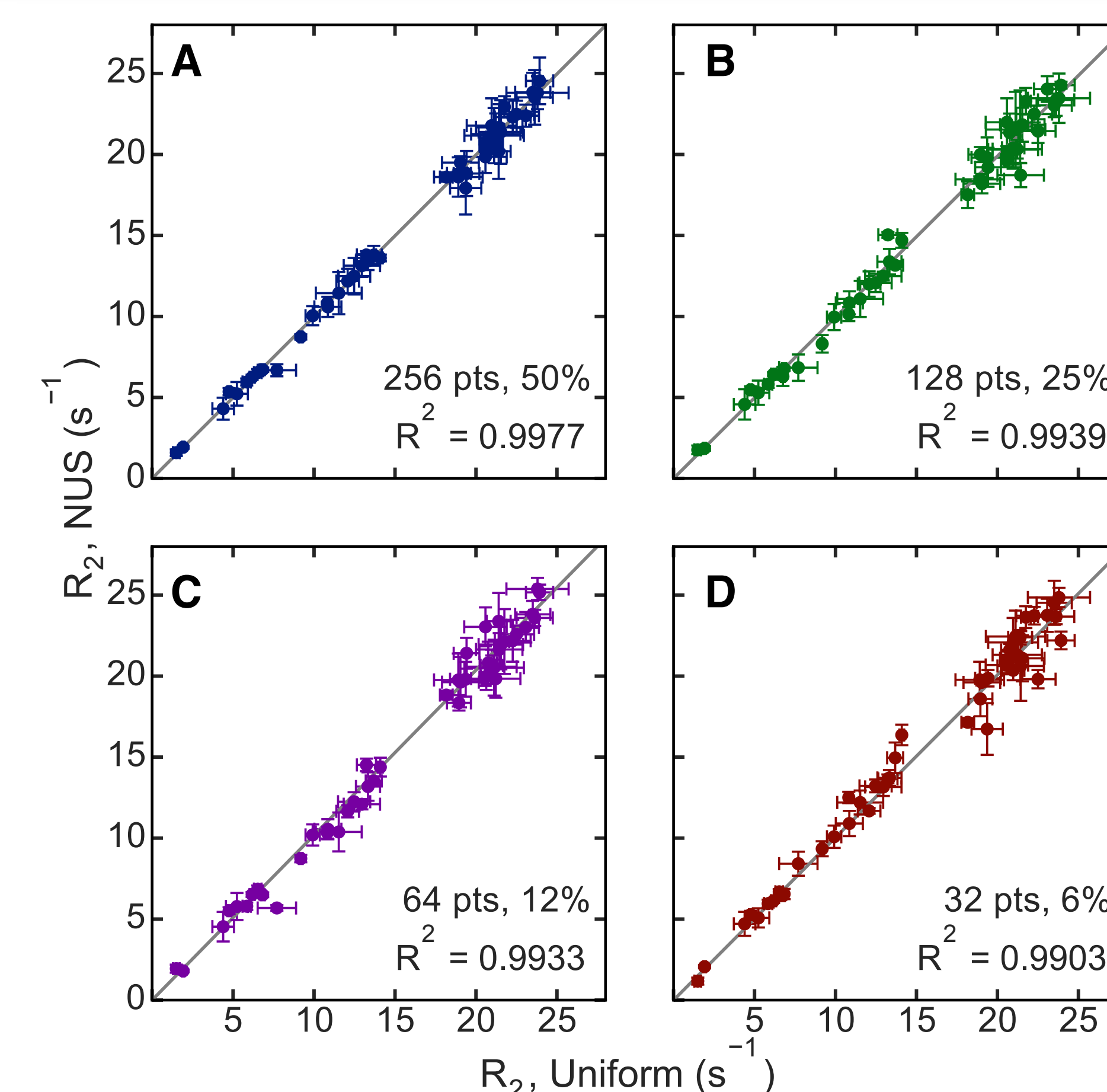


Figure 5. Correlation plots for the ^{15}N amide transverse relaxation rate constant (R_2) determined from NUS time series of different sampling densities relative to rates from uniformly sampled spectra. The plots contain (A) 256, (B) 128, (C) 64, and (D) 32 complex points, which correspond to 50%, 25%, 13%, and 6% sampling density, respectively.

Higher Dimensionality Spectra

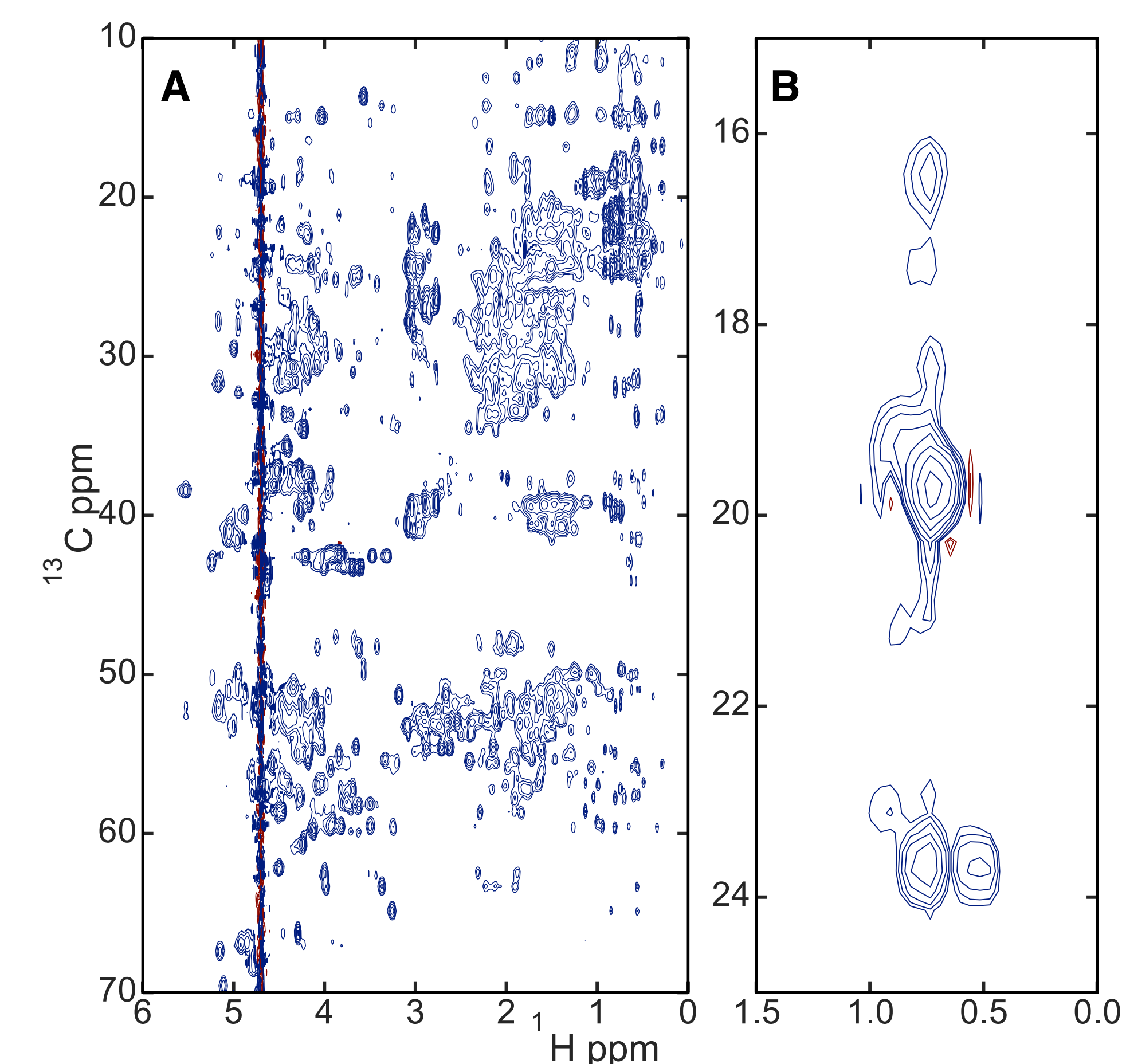


Figure 6. NESTA-NMR also processes higher dimensionality (3D and 4D) spectra. (A) The XZ projection from a 3D HCCH-TOCSY of U- ^{15}N , ^{13}C Ubiquitin with 6,000 complex points (37% sampling density) and (B) a ZA plane from a 4D CC-NOESY of U- ^{2}H , ^{15}N ^{13}C -ILV labeled ZA domain from ASAP1 with 12,000 complex points (8% sampling density).

Conclusions

- Gradient assisted virtual echo (GrAVE) is shown to greatly improve the fidelity of sparsely sampled, low dimensionality NUS spectra
- Using NESTA-NMR with GrAVE, ^{15}N amide transverse relaxation rates (R_2) can be determined with a high degree of accuracy for the *apo* form of GCN4 using spectra with as few as 32 complex points (6% sampling density)
- NUS-assisted acquisition of spin relaxation experiments is desirable for macromolecular systems with very sharp resonances, poor spectral resolution, or limited stability

NESTA-NMR can be downloaded from <http://nestanmr.com>
Documentation is available at <http://docs.nestanmr.com>

